Efficient enantioresolution of aromatic α-hydroxy acids with Cinchona alkaloid-based zwitterionic stationary phases and volatile polar-ionic eluents

Efficient enantioresolution of aromatic a-hydroxy acids with *Cinchona* alkaloid-based zwitterionic stationary phases and volatile polar-ionic eluents

Ina Varfaj [a,1], Michele Protti [b,1], Alessandro Di Michele [c], Alceo Macchioni [d], Wolfgang Lindner [e], Andrea Carotti [a,*], Roccaldo Sardella [a,f,*], Laura Mercolini [b]

[a] Department of Pharmaceutical Sciences, University of Perugia, Via Fabretti 48, 06123, Perugia, Italy

[b] Department of Pharmacy and Biotechnology (FaBiT), Alma Mater Studiorum, University of Bologna, Via Belmeloro 6, 40126, Bologna, Italy

[c] Department of Physics and Geology, University of Perugia, Via Pascoli 1, 06123, Perugia, Italy

d Department of Chemistry, Biology and Biotechnology, University of Perugia, Via Elce di Sotto 8, 06123, Perugia, Italy

[e] Department of Analytical Chemistry, University of Vienna, W€ahringer Strasse 38, 1090, Vienna, Austria

[f] Center for Perinatal and Reproductive Medicine, University of Perugia, Santa Maria Della Misericordia University Hospital, 06132, Perugia, Italy

* Corresponding author.
Department of Pharmaceutical Sciences, University of Perugia, Via Fabretti 48, 06123, Perugia, Italy.
E-mail addresses: andrea.carotti@unipg.it (A. Carotti), roccaldo.sardella@unipg.it (R. Sardella).
[1] Ina Varfaj and Michele Protti contributed equally to this work.

Highlights

- ZWIX(−) allows the enantioresolution of the three aromatic α-hydroxy acids.
- The optimized polar-ionic conditions are fully compatible with MS detectors.
- The developed LC method can be used to study biological matrices with MS detectors.
- Combining in silico simulations and ECD analyses is useful to derive the EEO.
- The retention mechanism can be explained with molecular dynamic simulations.

GRAPHICAL ABSTRACT

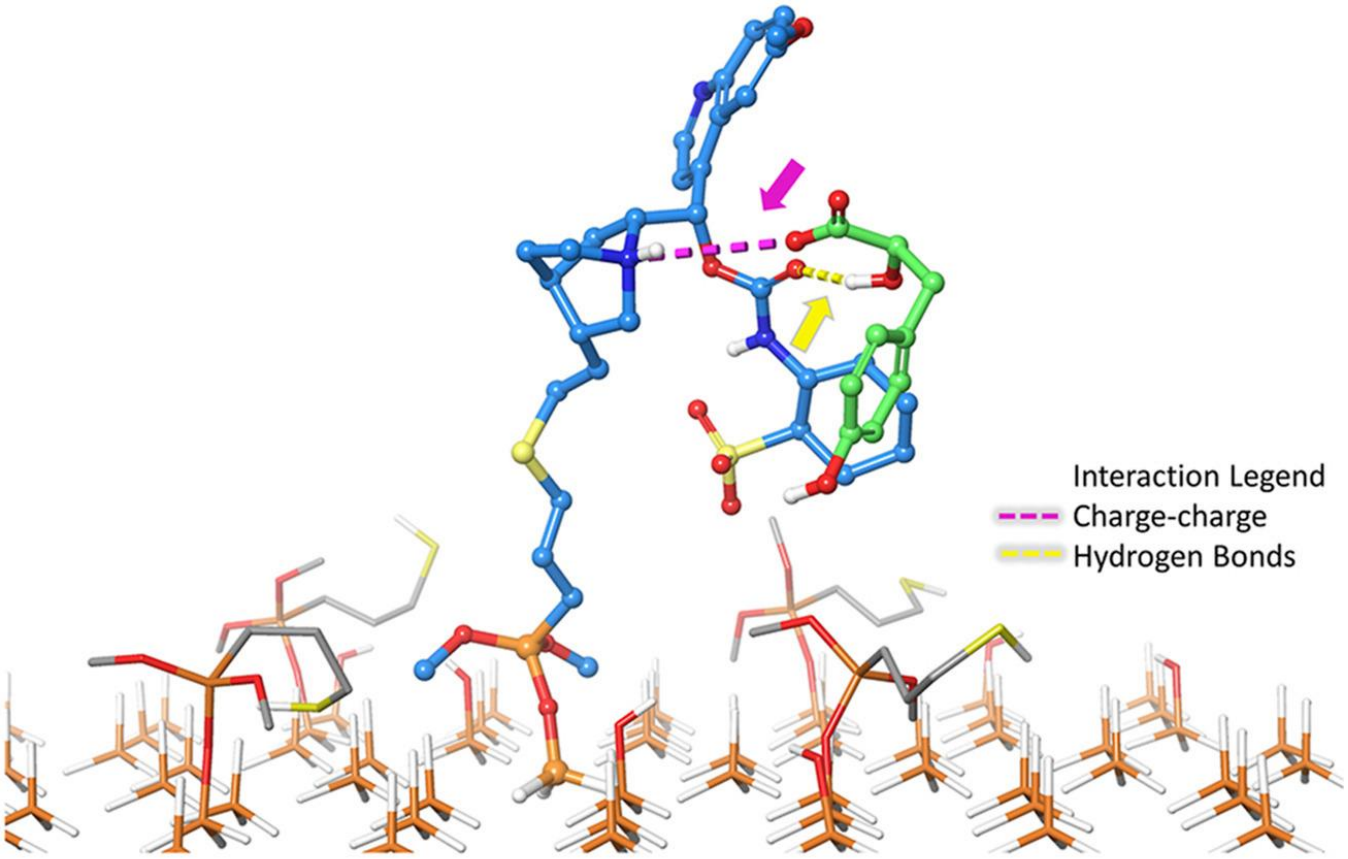

Interactions engaged by the CSP 1 (cyan sticks) and (*S*)-**3** (green sticks)

ABSTRACT

Single enantiomers of mandelic acid (1), 3-phenyllactic acid (2), and 3-(4-hydroxyphenyl)lactic acid (3) are the subject of many fields of investigation, spanning from the pharmaceutical synthesis to that of biocompatible and biodegradable polymers, while passing from the interest towards their antimicrobial activity to their role as biomarkers of particular pathological conditions or occupational exposures to specific xenobiotics. All above mentioned issues justify the need for accurate analytical methods enabling the correct determination of the individual enantiomers. So far, all the developed liquid chromatography (LC) methods were not or hardly compatible with mass spectrometry (MS) detection. In this paper, a commercially available Cinchona-alkaloid derivative zwitterionic chiral stationary phase [that is, the CHIRALPAK® ZWIX(−)] was successfully used to optimize the enantioresolution of compounds 1–3 under polar-ionic (PI) conditions with a mobile phase consisting of an acetonitrile/methanol 95/5 (v/v) mixture with 80 mM formic acid. With the optimized conditions, enantioseparation and enantioresolution values up to 1.46 and 4.41, respectively, were obtained. In order to assess the applicability of the optimized enantioselective chromatography conditions in real-life scenarios and on MS-based systems, a proof-of-concept application was efficiently carried out by analysing dry urine spot samples spiked with 1 by means of a LC-MS system. The (S)<(R) enantiomer elution order (EEO) was established for compounds 1 and 2 by analysing a pure enantiomeric standard of known configuration. This was not possible for 3 because not commercially available. For this compound, the same EEO was identified applying a procedure based on ab initio time-dependent density-functional theory simulations coupled to electronic circular dichroism analyses. Moreover, a molecular dynamics simulation unveiled the role of the phenolic OH in compound 3 in the retention mechanism.

KEYWORDS:

Ab-initio simulations; Aromatic α-hydroxy acids; Dry urine spots; Electronic circular dichroism; Enantioresolution; MS-Compatible conditions.

INTRODUCTION

Mandelic acid (1), 3-phenyllactic acid (2), and 3-(4-hydroxyphenyl)lactic acid (3) (Fig. 1) are aromatic α-hydroxy acids, with compounds 2 and 3 belonging to the class of phenyl propionic acids.

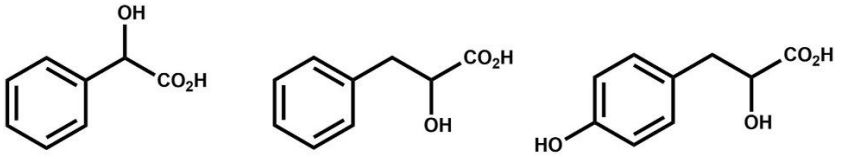

1 2 3

Fig. 1. Structure of the compounds investigated in the study: (1) mandelic acid; (2) 3-phenyllactic acid; (3) 3-(4-hydroxyphenyl)lactic acid.

Single enantiomers of compounds 1–3 are versatile chiral building blocks for the large-scale production of numerous active pharmaceuticals ingredients including semi-synthetic penicillins, cephalosporins and other antibiotics [[1], [2], [3], [4]], antitumor [5,6] and antiobesity agents [7], just to cite some. The three molecules are also very well-known (in an enantiomerically specific manner) for their antimicrobial activity [8,9], as well as for their use in the synthesis of biocompatible and biodegradable polymers also for promising biomedical applications [10,11].

Various approaches have been developed so far for the preparation of the enantiopure form of compounds 1–3. These approaches include traditional organic synthesis methods, as well as enzymatic and biological routes [9,12,13]. In this scenario, over the last two decades, both biocatalytic asymmetric synthesis and fermentation processes have gained great interest both in industry and academia owing to the high efficiency, simple operation, environment-friendly nature and, in particular, excellent stereoselectivities [9,12,13]. Also importantly, the enantiomers of compounds 1–3 are often measured in biological matrices such as plasma and urine as biomarkers of particular pathological conditions (including phenylketonuria, hyperphenylalaninemia, tyrosinemia, gut microbial alterations, etc.) [14,15] as well as of environmental and occupational exposures to specific xenobiotics (such as styrene and ethylbenzene) [[16], [17], [18]].

All above mentioned issues justify the need for accurate analytical methods enabling the correct determination of the individual enantiomers. So far, various direct enantioselective chromatography methods with commercially available chiral stationary phases (CSPs) have been developed for this aim. Accordingly, efficient enantioselective liquid chromatography (LC) analyses were performed with polysaccharide- [9,[19], [20], [21], [22]], glycopeptide- [23,24], protein- [25] and ligand-exchange-based [26] CSPs. However, all these methods were not or hardly compatible with mass spectrometry (MS) detection.

In order to fulfil this gap, we have developed the first LC method fully compatible with MS detectors. This

efficient enantioselective LC method relies upon the use of a polar-ionic (PI) mobile phase in combination with a zwitterionic CSP operating as an anion-exchanger. This zwitterionic CSP (CSP 1, Fig. 2) consists of a Cinchona-alkaloid derivative type chiral selector (SO), which has proven to produce enantioselecivity for many ionic and ionizable analytes under the most relevant elution regimes for LC applications [[27], [28], [29]]. Since commercial enantiopure standards are unavailable for compound 3, its enantiomeric elution order (EEO) in the optimized mobile phase conditions has been obtained with the application of a well-established method based on ab initio time-dependent density-functional theory (TD-DFT) simulations coupled to electronic circular dichroism (ECD) analyses [30,31]. Finally, in order to prove the compatibility of our method with MS detectors, dried urine spot (DUS) microsamples [32,33] spiked with mandelic acid (1) have been extracted and efficiently analysed by means of an ultra-high performance liquid chromatography (UHPLC)-MS system exploiting the optimized enantioselective chromatography conditions.

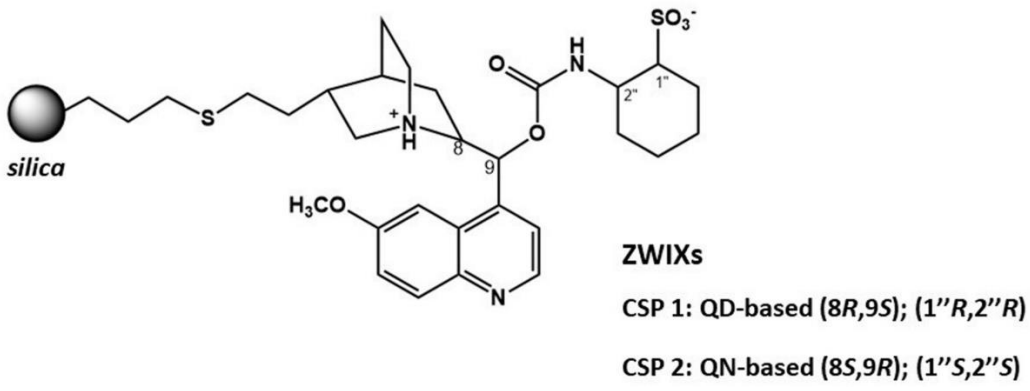

Fig. 2. Structure of zwitterionic CSPs operating according an ion-exchange mechanism. The two CSPs belong to the family of Cinchona alkaloid-based enantiorecognition materials and are commercialized by Chiral Technology Europe (Strasbourg, France) under the trade names CHIRALPAK® ZWIX(−) (CSP 1) and CHIRALPAK® ZWIX(+) (CSP 2).

2. MATERIAL AND METHODS

2.1. Chemicals

All the reagents and solvents used in the study were of analytical grade. Acetonitrile (ACN), methanol (MeOH), formic acid (FA), acetic acid (AcOH), as well racemic mandelic acid (1), 3-phenyllactic acid (2), 3-(4-hydroxyphenyl)lactic acid (3) and 3-phenylpropionic acid - used as internal standard (IS) - were purchased from Merck Life Science (Merck KGaA, Darmstadt, Germany). The pure enantiomer of 1 and 2 were also from Merck Life Science. Water for HPLC analysis was purified with a New Human Power I Scholar water

purification system (Human Corporation, Seoul, Korea). For UHPLC-MS analysis, MS-grade ACN, MeOH and FA were employed and were purchased from Merck Life Science. Whatman FTA™ DMPK-B IND cards for DUS sampling were purchased from Merck Life Science, while a Whatman (Maidstone, MA, USA) Harris Uni-Core Punch, 6.0 mm was used for punching the DUS discs out of the spotting cards.

2.2. Instrumentations

The HPLC-UV analyses were performed on a Shimadzu HPLC equipped with a SCL-10Avp system controller, two LC-10AD high pressure binary gradient delivery systems, a SPD-10A variable-wavelength UV–Vis detector, and a Rheodyne 7725i injector with a 20 µL stainless steel loop. The enantioselective analyses were carried out with the CHIRALPAK® ZWIX(−) (CSP 1, Fig. 2) and CHIRALPAK® ZWIX(+) (CSP 2, Fig. 2) (150 mm × 4.0 mm I.D, 120 Å pore size, 3 µm particle diameter) columns kindly provided by Chiral Technologies Europe (Strasbourg, France). All the analyses were performed at a 0.2 mL min−1 eluent flow rate. The column temperature was fixed at 25 °C with a Grace (Sedriano, Italy) heather/chiller (Model 7956R) thermostat. A 254 nm detection wavelength was selected for the analyses. Acetone was selected as the unretained marker to evaluate the chromatographic parameters.

An ultra-high performance liquid chromatography coupled to single-quadrupole mass spectrometry (UHPLC-MS) system was exploited in order to assess the applicability of the optimized enantioselective chromatography conditions on MS-based systems and to obtain a proof-of-concept application by analysing spiked DUS samples. The system was composed of a UHPLC Vanquish pump, Vanquish Autosampler, Vanquish column compartment, and ISQ EC single-quadrupole mass spectrometer (Thermo Fisher Sci., Waltham, MA, US), while data elaboration was carried out by means of Thermo Fisher Scientific Dionex Chromeleon 7.3 Chromatography Data System software. Enantioselective separations were obtained on the same CHIRALPAK® ZWIX(−) (CSP 1) column previously described, a 0.2 mL min−1 flow rate and 20 µL injection volume; the autosampler needle was washed with 10% (v/v) MeOH (10 s) after each sample injection. Isocratic mobile phase consisted of a mixture of ACN/MeOH 95/5 (v/v) with 80 mM FA. Optimized mass spectrometric parameters were the following: vaporizer temperature (VT), 117 °C; ion transfer tube temperature (ITT), 300 °C; sheath gas pressure (SGP), 30 psig; auxiliary gas pressure (AGP), 3 psig; sweep gas pressure (SWGP), 0.5 psig. Negative ionisation mode was exploited, which resulted in extracted mandelic acid (1) chromatograms at m/z 151.1. Column and autosampler temperatures were maintained at 25 °C and 10 °C, respectively.

The ECD spectra were recorded by a Jasco J-810 Spectropolarimeter (Jasco Corporation, Tokyo, Japan) at 25 °C, using 10 mm quartz cell. The samples were solubilized in MeOH and analysed in the global spectral range of 210–400 nm.

2.3. Computational studies

2.3.1. Theoretical ECD spectra simulations

Compounds 1–3 were built by the Maestro interface (Schrödinger, LLC, New York, NY, 2020) present in the Schrödinger Suite 2020-2; Ligprep Protocol set at the default options was adopted to assign the correct protonation state. MMFF94s force field was used to perform a conformational search with the MacroModel module (Schrödinger, LLC, New York, NY, 2020) executing 200 steps with the "Mixed torsional/Low-mode sampling" using water as solvent and retaining at most 50 conformers, lying in a window of 5.0 kcal mol−1 from the global minimum energy. The torsional sampling involved either multiple Monte Carlo minimum searches for global exploration, and the low mode conformational search allowed for automatic local exploration. The conformers that exceeded the threshold of 0.5 Å of the maximum atom deviation for any pair of corresponding atoms were considered to be different. Using the same settings applied in a recently published paper to simulate the ECD spectra of compound 1 [34], the resulting conformers were all submitted to a quantum mechanical energy optimization using the wB97X-D as DFT and the 6–311++G∗∗. Finally, the level of accuracy was set to Ultrafine (iacc = 1) in the Jaguar module (Schrödinger, LLC, New York, NY, 2020) [[35], [36], [37], [38]]. A RMSD threshold value of 0.01 Å for heavy atoms was applied to eliminate the high-lying or redundant conformers. The theoretical chiroptical properties of all the compounds were determined using a standard protocol for stereochemical characterization using TD-DFT calculations [30]. The sTD-DFT [39] calculations were carried out using the ORCA 4.1.2 software [40] using the wB97X-D3 as DFT and the 6–311++G∗∗ basis set. The 50 lowest energy electronic transitions of each optimized conformer were used to calculate the theoretical values of oscillator strength (fj), rotational strength in dipole velocity formalism (Rj), and excitation energy (expressed as wavelength, j). By approximation of fj and Rj values to Gaussian bands with a σ value of 0.3 eV [41] the theoretical spectra of the optimized conformers were then derived. The weighted average of the contribution of all conformers according to their Boltzmann equilibrium populations at 298.15 K and 1 atm, based on free energy values (G), was used to derive the theoretical ECD spectra of the compound and compared to the experimental spectra. This last step was performed using the SpecDis software [42]. The in silico spectra obtained by the different basis set used were compared with the experimental outcome, and the one showing the most similar profile was then selected for the EEO determination.

2.3.2. Molecular dynamics simulations

The Maestro interface (Schrödinger, LLC, New York, NY, 2020) present in the Schrödinger Suite 2020-2 was used to reproduce the chromatographic environment. As reported in the previous work [43], a cubic box

was built with a 30 Å side length. For a realistic reproduction of the stationary phase environment, four 3-mercaptopropyl-functionalized silanols (~1.97 mol m−2), eight free silanols (~8.0 mol m−2) and forty-five silicon atoms were considered for each grafted selector (SO) unit (~0.5 mol m−2), at the base of the box. All the silicon atoms in the base layer were set frozen during the molecular dynamics. The box was solvated with ACN/MeOH 95/5 (v/v). The simulations were performed in the canonical ensemble at 298 K. The temperature in the simulation cell was maintained constant through use of a Nosé-Hoover thermostat [44,45]. All the other parameters in the simulation study were left to default values in the Desmond Molecular Dynamics System present in the Schrödinger Suite 2020-2 [46]. The production run produced 1000 frames during the 300 ns dynamics, with an integration time of 2 fs.

2.4. Preparation of dry urine spots (DUSs) and UHPLC-MS analysis

Urine samples, used as blank matrix, were obtained from healthy volunteers. Aliquots of 200 µL were spiked with 10 µL of standard mixtures containing 1 and IS to obtain urine concentrations of 100 ng mL−1, 1 µg mL−1 and 100 µg mL−1 of 1 and a fixed IS concentration of 100 ng mL−1. Then, the obtained fortified urine was subjected to DUS sampling and pretreatment before UHPLC-MS analysis. Aliquots of 10 µL of urine were transferred onto a Whatman FTA™ DMPK-B IND card by means of micropipetting; the obtained spots were left to dry for 1 h at room temperature, then stored in the dark with suitable desiccant until pretreatment and analysis. At the time of analysis, a 10-mm diameter circle was punched out from the card with a puncher and placed into a vial with 250 µL of 80 mM FA in MeOH, subjected to ultrasound-assisted extraction (UAE) at room temperature for 10 min and centrifuged at 4000 rpm for 5 min at 4 °C. The supernatant was brought to dryness under a gentle N2 stream, re-dissolved with 100 µL of an ACN/MeOH 95/5 (v/v) mixture with 80 mM FA and analysed by UHPLC-MS without the need for further treatment. Resulting chromatograms were checked and compared with chromatograms from 1 standard solutions, then the overlapping of retention times and the correspondence of chromatographic parameters were verified.

3. RESULTS AND DISCUSSION

3.1. Enantioseparation study of compounds 1–3

One of the main advantages of using CSP 1 and CSP 2 (Fig. 2) is their well-documented flexibility to behave as cation-exchangers (CXs) for the enantioseparation of chiral bases [47,48], as anion-exchanger (AXs) for the enantioseparation of chiral acids [27,49,50], and as zwitterionic ion-exchangers for the enantioseparation of ampholytic compounds [28,51,52].

CSP 1 and CSP 2 are commercially available as CHIRALPAK® ZWIX(−) and CHIRALPAK® ZWIX(+) (Chiral

Technology Europe, Strasbourg – France), and present the following structural characteristics: in CSP 1, QD is fused via a carbamoyl group with (R,R)-trans-2-aminocyclohexanesulfonic acid (R,R-ACHSA), whereas in CSP 2 QN is identically fused with (S,S-ACHSA); for the chiral selectors (SOs) incorporated in CSP 1 and CSP 2, the absolute configuration of N1, C3 and C4 is the same (that is, 1S,3R,4S), while an opposite configuration is present at C8 and C9 of the Cinchona scaffold (that is, 8R, 9S in CSP 1, and 8S, 9R in CSP 2). Moreover, CSPs 1 and 2 feature opposite configuration also at C1" and C2" in the ACHSA ring, which is the reason why these two CSPs very often display a so-called "pseudo-enantiomeric" behaviour in terms of their chiral recognition ability [49,[53], [54], [55]].

The use of polar-ionic (PI) eluents was here preferred over reversed-phase (RP) ones since the former often produce higher enantioselectivities as a result of the following mechanisms. PI mobile phases are capable to attenuate or even inactivate non-enantioselective interactions (both hydrophobic and other types of interactions) with the stationary phase functionalities [52,54,56]. Moreover, a strong solvation of ionic selectands (SAs) and zwitterionic SOs takes place under RP conditions, which in turn reduces the strength of the ion pairing process with a detrimental effect on enantioselectivity. Furthermore, the solvation by aqueous eluents might mitigate or even abolish non-ionic but stereo discriminating interactions, with a negative impact on the overall enantioselectivity extent.

Due to the IMCI effect, the elution of anionic analytes might in principle occur even without any mobile phase counterion [28]. However, this possibility is disadvantageous in practice since it may lead to extremely long retention times [28]. Therefore, acidic additives (often used in combination with basic additives or replaced by buffers) are added to the eluent as counter-ions to trigger the enantioseparation process. The incorporation of acids in the eluent ensures, inter alia, the protonated state of the quinuclidine nitrogen, which is a fundamental pre-requisite for the ion-pair and ion-exchange processes.

A solution consisting of MeOH with 160 mM AcOH was used as initial mobile phase. The use of the highly volatile and more MS compatible FA was avoided for its well-known relatively fast reaction with MeOH yielding FA methyl ester [52,56]. With that mobile phase and CSP 1, only compound 1 was partially separated (Fig. 3A), while base-line resolution was obtained for compounds 2 and 3 (Table 1, entries 1, 8 and 10). CSP 2 did not distinguish the enantiomers of 1, while exhibited good enantioseparation capability for the other two analytes (data not shown). The two zwitterionic SOs are diastereomeric in nature and therefore characterized by geometrically and conformationally oriented interaction sites, such as the carbamate group (mostly involved in H-bonding- and dipole-dipole-interactions) and the quinoline moiety (mostly participating in π-π-interactions). These structural elements are together or separately involved in the overall enantiorecognition process. The different chromatographic behaviour exhibited by CSP 1 and CSP 2 can be rationally explained on this basis [47]. CSP 1 was therefore selected for the following

optimization steps aimed at improving the performance on compound 1.

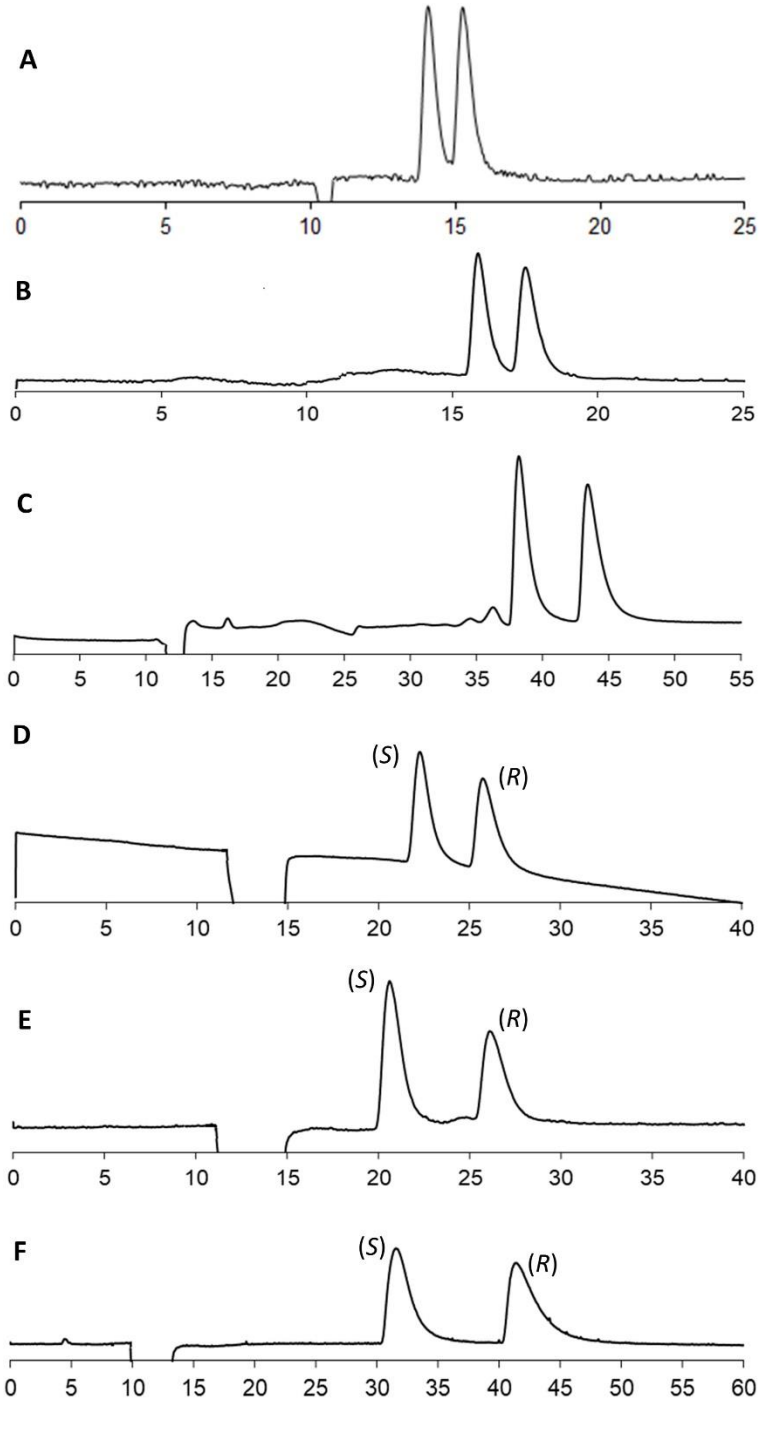

Fig. 3. Chromatograms of compounds 1–3 obtained under PI conditions with CSP 1. Mobile phase conditions can be retrieved from Table 1 (A) cpd 1, entry 1; (B) cpd 1, entry 2; (C) cpd 1, entry 6; (D) cpd 1, entry 8; (E) cpd 2, entry 10; (F) cpd 3, entry 12. The EEO has been reported in the best chromatographic conditions.

Table 1. Chromatographic performances obtained for compounds 1–3 with CSP 1.

Compound	Entry	Mobile phase[a]	Chromatographic parameters					
			k_1	k_2	N_1	N_2	α	R_S
1	1	A	0.74	0.89	4568	4422	1.20	1.37
	2	B	0.96	1.17	4466	4059	1.21	1.59
	3	C	0.83	1.01	3354	2655	1.23	1.32
	4	D	0.91	1.13	4314	4024	1.24	1.74
	5	E	1.45	1.72	4514	4280	1.19	1.73
	6	F	3.73	4.37	6354	5398	1.17	2.44
	7	G	2.95	3.68	873	454	1.25	1.04
	8	H	1.76 (*S*)	2.18 (*R*)	3092	2862	1.24	1.97
2	9	A	0.37	0.77	2438	2793	2.06	3.23
	10	H	1.55 (*S*)	2.23 (*R*)	1982	2283	1.44	2.72
3	11	A	0.27	0.65	3159	3179	2.39	3.64
	12	H	2.90 (*S*)	4.12 (*R*)	1447	1688	1.42	2.69

[a] Composition: (a) MeOH with 160 mM AcOH; (b) MeOH with 80 mM AcOH; (c) MeOH/ACN 98/2 (v/v) with 80 mM AcOH; (d) MeOH/ACN 95/5 (v/v) with 80 mM AcOH; (e) MeOH/ACN 90/10 (v/v) with 80 mM AcOH; (f) ACN with 80 mM AcOH; (g) ACN/MeOH 95/5 (v/v) with 80 mM AcOH; (h) ACN/MeOH 95/5 (v/v) with 80 mM FA. The EEO has been reported in the best chromatographic conditions.

Testing different additive concentrations can be a useful tool to adjust column performance, e.g., to slow analysis with improved enantioresolution. When AcOH concentration was reduced from 160 mM (Table 1, entry 1) down to 80 mM (Table 1, entry 2), retention factors significantly increased in accordance to a typical AX process [27,49] and the stoichiometric displacement model [28,51,[56], [57], [58]]. At the same time, the α value remained nearly unchanged, suggesting a negligible effect of counterion on other tentative binding increments mainly responsible for enantioselectivity (namely H-bond and van der Waals/steric interactions). Instead, resolution factors (RS) increased with the reduction of the eluent ionic strength, as a result of the increased retention of both enantiomers. With the lower AcOH concentration, base-line separation (RS of 1.59; Table 1, entry 2) (Fig. 3B) of 1 was obtained.

In order to further improve the chromatographic performance, we scrutinized the impact of the combination of a protic and an aprotic eluent component. Accordingly, we continued to use MeOH as a protic solvent (which can suppress H-bonding interactions), this time in combination with a low amount of

ACN, which is an aprotic solvent known to support ionic interactions but to interfere with aromatic (π-π-stacking) interactions [59]. In order to optimize the ratio of these two solvents, three different binary eluents were evaluated (Table 1, entries 3–5), while keeping the AcOH concentration fixed at 80 mM. As expected, a clear increase of the retention was observed with increasing concentrations of ACN from 2 up to 10% (v). This behaviour can be explained by considering the reduced solvation power of ACN leading to the enforcement of the electrostatic interactions between the anionic group of the analyte and the protonated quinuclidine moiety of the SO. However, the presence of an aprotic component in the eluent did not significantly enhance the separation properties of the system (Table 1, entries 3–5), thus indicating that H-bonding interactions are important for analyte retention, whilst these seem not to support the chiral recognition process. Conversely, increasing the ACN concentration in the eluent led to an improvement of RS values as a result of the higher retention and enhanced efficiency.

Replacing MeOH with ACN, while keeping constant the acid concentration in the eluent, led to the formation of a thinner solvation shell around the charged moieties of both SO and SA, thus amplifying the strength of the electrostatic attractions, with a consequent elongation of the retention time (Table 1, entries 2 and 6) [28,47,49,55,60]. The longer retention times recorded with the aprotic mobile phase can be plausibly attributed to a less effective contribution of the IMCI effect. This outcome is in strict accordance with the recognized ability by ACN to promote stronger intermolecular SO-SA interactions disfavouring intramolecular interactions. A mobile phase consisting of only ACN (plus ionic additives) is usually not recommended as it reduces the solubility of many ionizable solutes. As a consequence, these compounds could partially precipitate on the top of the column and a slow dissolution of this portion of solute takes place only with the passage of large volumes of mobile phase. Severe peak tailing is often promoted in such circumstances. This might explain the stronger peak asymmetry observed with the ACN- (tailing factor measured at 10% of peak height equal to 2.2 and 2.4 for the first and the second eluted enantiomer, respectively; Fig. 3C) over the MeOH-based (tailing factor measured at 10% of peak height equal to 1.7 for both enantiomers; Fig. 3B) eluent. The stronger tailing observed with ACN was accompanied by the remarkable gain in resolution (Table 1, entries 2 and 6), ascribable to the higher retention and improved efficiency. Based on this result, and aimed at reducing the elution time while keeping safe the quality of the enantioseparation process, also in terms of peak shape, 5% (v) of MeOH was added to ACN with AcOH (80 mM). With this eluent system an expected reduction of the retention time turned out along with a sensitive deterioration of the kinetic properties of the system (Table 1, entry 7). Following this observation, and aware that the type and concentration of acidic additive can have a profound impact on the retention profile and the quality of the enantioseparation process [27,50,55], AcOH was replaced with FA at the same concentration (80 mM). With this eluent, no problems with mobile phase stability actually exist due to the

high content of ACN, making the mobile phase more suited to MS detection systems. In the last eluent, excellent chromatographic performances were obtained for compound 1 (Table 1, entry 8; Fig. 3D), which stimulated us to test these conditions also for the analysis of 2 and 3. Also for these two compounds, very successful results were obtained under the last PI eluent tested (Table 1, entries 10, and 12; Fig. 3E and 3F, respectively for compound 2, and 3).

It has been recently documented [59] that FA and AcOH can differently contribute to the overall enantiorecognition event with the CSPs employed in this study. Indeed, these two acids have been demonstrated to participate differently in the formation and composition of the solvation shells of the CSPs and SAs. In spite of their non-chiral nature, the acidic additives display an intimate participation to the chromatographic process as a whole. Indeed, these additives are capable to affect the conformation of the SO and SA, in turn modifying the orientation of the complementary interacting functional groups on SO and SA. The higher retention in the presence of AcOH (Table 1, entry 7) over FA (Table 1, entry 8) can be explained with the ability by the former to produce solvation shells of smaller dimension on CSP 1, ultimately leading to a stronger Coulomb attraction and higher enantiomer retention [59]. On the other side, the highly polar FA is better adsorbed onto the CSP surface, thereby implying a remarkable change of its retention properties.

The poor kinetic properties produced by eluent “g” (Table 1, entry 7) can be tentatively explained by a competition between AcOH and MeOH in the solvation layer of the CSP, which can impair the conformational flexibility of the SO unit [59].

Very intriguingly, a rather different chromatographic behaviour was found for all of the three compounds when solubilized in ACN and analysed with the optimal [ACN/MeOH 95/5 (v/v) with 80 mM FA] mobile phase. A sensitive reduction of the retention time was always observed, accompanied by very appreciable enantioseparation and enantioresolution factors (Fig. 4). In a previous paper [61], some of us already highlighted that the sample diluent may have a deep effect on the enantioseparation profile with ZWIX-type CSPs under PI elution conditions. Ideally, for Chiralpak ZWIXs used under PI condition, the sample diluent should have low elution strength, and therefore plain ACN should theoretically represent one of the best options. However, further investigations are required to rationalize the effect produced by ACN as sample diluent, which is out of the scope of the present paper.

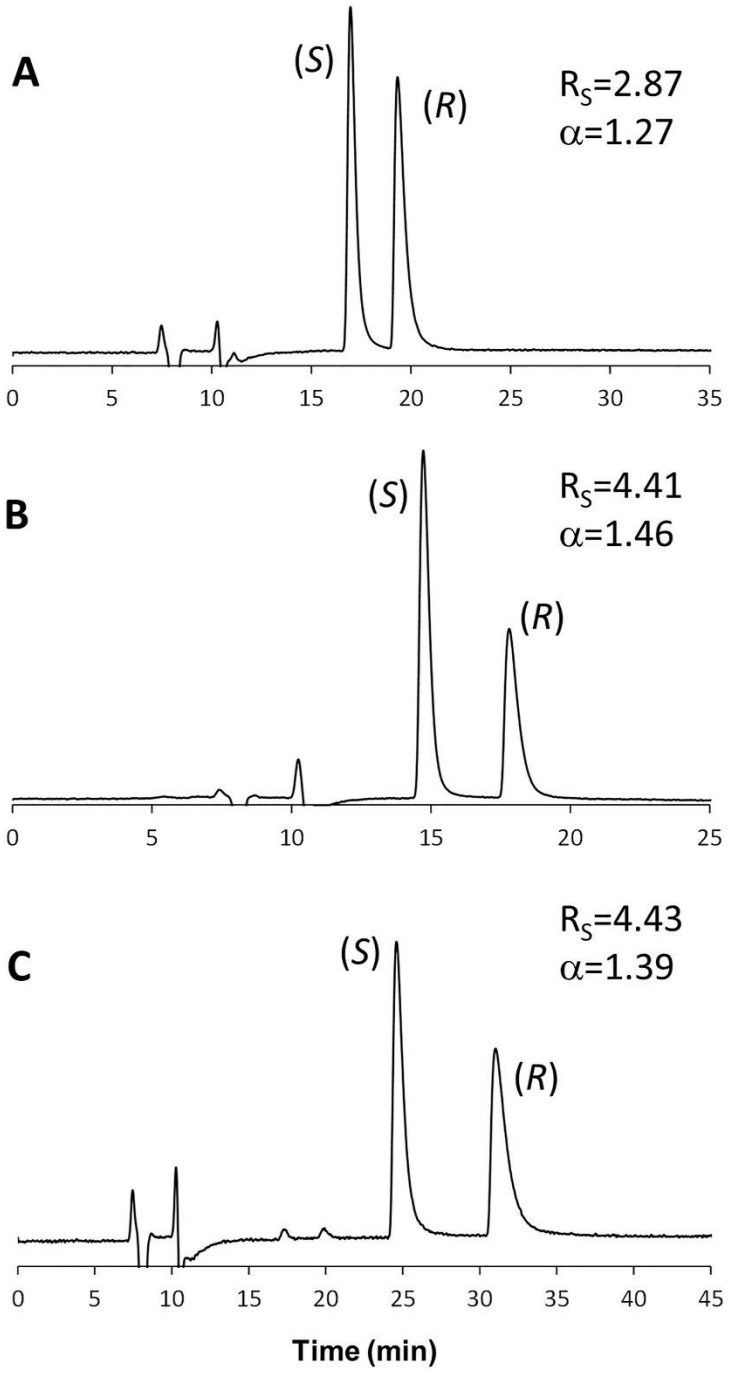

Fig. 4. Chromatograms of compounds (A) 1, (B) 2, (C) 3, obtained with the optimal [ACN/MeOH 95/5 (v/v) with 80 mM FA] mobile phase after the solubilization in plain ACN.

The higher retention of compound 3 under the applied eluent conditions with CSP 1 can be tentatively explained with a stabilizing H-bonding interaction by the phenolic OH group (see section 3.2. for further details).

The chromatogram of 2 depicted in Fig. 3E reveals the non-racemic nature of this analyte, although it was purchased as such. The analysis of this compound was performed under the same eluent conditions with CSP 2 in order to verify this issue. Thanks to the pseudo-enantiomeric behaviour often exhibited by the two zwitterion-type CSPs, a reversal of the elution order was observed for compound 2 when analysed with the CSP carrying the quinine scaffold (Fig. S1, Supplementary Material). The scalemic nature of sample 2 was tentatively ascribed to an incorrect storage of the sample powder in our laboratory.

Mobile phase "h" was also used in combination with CSP 2. As a result, only compound 2 was almost base-line separated, while a hint of separation turned out for 1 and co-elution for the enantiomers of 3.

The (S)<(R) enantiomer elution order (EEO) was established for compounds 1 and 2 injecting a pure enantiomeric standard of known configuration. This was not possible for 3 because not commercially available. For this compound, the same EEO was identified applying a well-established molecular modelling procedure described in detail in sections 2.3 Computational studies, 3.2 Assignment of the absolute configuration through ECD studies and molecular dynamics simulations.

3.2. Assignment of the absolute configuration through ECD studies and molecular dynamics simulations

Due to the lack of pure enantiomeric standards of known stereochemistry for compound 3, an indirect protocol was applied to establish the enantiomer elution order (EEO) under the optimized eluent conditions. Accordingly, based on a well-established protocol [30,31], ECD studies were coupled to ab initio TD-DFT simulations. Experimental ECD spectra of the two enantiomers of compound 3 after their off-line collection with the CSP 1 have been retrieved.

As readily evident from the ECD spectra displayed in Fig. 5, the two isolated peaks exhibit specular Cotton effects typical of enantiomeric compounds, with the main band centred at around 230 nm. The ECD spectrum of the first eluted peak is well mimicked by the TD-DFT theoretical spectrum of (S)-3 obtained by the use of the wB97X-D functional with the 6–311++G∗∗ basis set.

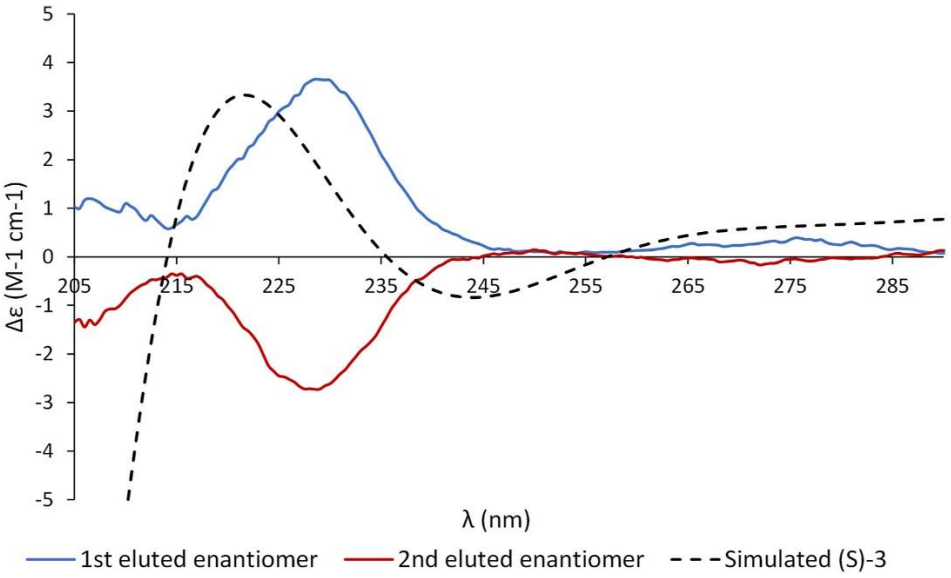

Fig. 5. Experimental ECD spectra of the first- (blue line) and second-eluted (red line) enantiomeric fraction of 3. The theoretical spectrum of the (S)-enantiomer is reported as black dashed-line. (For interpretation of the references to colour in this figure legend, the reader is referred to the Web version of this article.)

In order to confirm the correctness of the sTD-DFT settings used for the assignment of the EEO of compound 3, the same protocol was also applied to calculate the theoretical ECD spectrum for the enantiomers of compounds 1 and 2 (Fig. S2, Supplementary Material). The ECD spectra of compounds 1 and 2 confirmed that the employed computational method is capable to successfully reproduce the Cotton effects for these two compounds. Moreover, the results obtained for the enantiomers of 1 and 2 are in strict accordance with those produced by other authors [34,62], in turn confirming the quality of our approach any longer.

The main positive Cotton effect at around 230 nm, that is a shared signature of the ECD spectra of both compounds 1 and 2, is also evident in the theoretical spectrum of (S)-3, supporting a safe conclusion about the EEO. Based on this result, the (S)-3 < (R)-3 can be deduced.

With respect to compounds 1 and 2, analyte 3 bears a unique feature that is a para-hydroxy moiety that was found to play a role in the retention mechanism. In order to investigate this aspect and with the additional aim to further support the indirect EEO assignment, a molecular dynamic run has been performed on both (S)- and (R)-3 enantiomers using a simulation box representing the chromatographic environment, as described in details in section 2.3.2. The monitoring of the H-bond established by the hydroxy group during the whole trajectory revealed that (R)-3 enantiomer interacts 48 times with the sulfonic acid moiety of the ZWIX(−) while the (S)-3 molecule only three times engages a hydrogen bond

with the methoxy group of the quinoline moiety of the selector (Fig. 6A and B, respectively). The obtained results are in line with the retention behaviour of this compound over the other two examined.

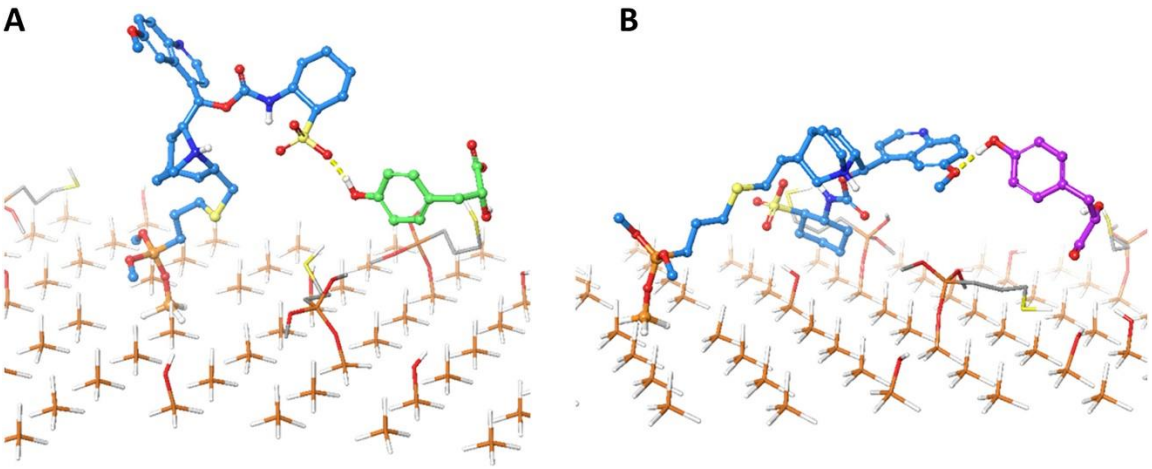

Fig. 6. Exemplary frames of the H-bond interactions (yellow dashed lines) engaged by the CSP 1 (cyan sticks) and (A) the (S)-3 (green sticks) and (B) (R)-3 (magenta sticks). (For interpretation of the references to colour in this figure legend, the reader is referred to the Web version of this article.)

3.3. Dried urine spot (DUS) analysis

In order to assess the applicability of the optimized enantioselective chromatography conditions in real-life scenarios and on MS-based systems, a proof-of-concept application was carried out by analysing DUS samples spiked with mandelic acid (1) by means of a UHPLC-MS system. Details on this subject are reported in section 2.4.

For this proof-of-concept application, it should be considered that, for the occupational exposure to styrene, the Biological Exposure Index (BEI) for mandelic acid is 800 mg g−1 creatinine (corresponding to a concentration of mandelic acid of 8 µg mL−1 urine, considering an average urinary creatinine concentration of 1 mg dL−1), according to the American Congress of Governmental Industrial Hygienists (ACGIH) [63]. On the other hand, physiological concentrations of mandelic acid in urine samples from workers not exposed to styrene were estimated to be in the order of magnitude of 25–250 ng mL−1 [64].

In the present study, method sensitivity in terms of lower limit of quantitation (LLOQ) was evaluated based on international bioanalytical method validation guidelines [65] as the lowest concentration of 1 in DUS samples which can be quantified reliably, with an acceptable accuracy and precision, and corresponding to 5 times the signal of a blank sample. The LLOQ value estimated for the methodology proposed herein was 5 ng racemic 1 per mL urine, thus being well below the BEI limit value but also lower than physiological 1

urinary levels in non-exposed workers.

In Fig. 3S (Supplementary Materials), the ESI-UHPLC-MS chromatogram obtained from the analysis of a DUS sample spiked with rac-1 is shown.

4. CONCLUSIONS

In this paper we have demonstrated that the Cinchona-alkaloid derived zwitterionic CSPs are suitable materials for the enantioresolution of the three aromatic α-hydroxy acids under investigation. The optimized chromatographic method based on the use of a volatile PI mobile phase makes it compatible with MS detection systems. The possibility to perform analysis by means of mass spectrometry opens the way to carry out important in-depth investigations in crucial fields such as biomarker and environmental monitoring and food safety assessment, just to cite some. In this framework, the possibility to combine the developed advanced chromatographic system to automated microsampling protocols and platforms for ultra-high performance liquid chromatography coupled to mass spectrometry analysis can make it easier to set-up high-throughput screening campaigns. This last point can be concretely pursued thanks to the possibility to efficiently scale the developed chromatographic method down to the same commercial columns of smaller dimensions.

Based on the encouraging results obtained in the present study, we intend to apply the developed method for the following purposes. The optimized chromatographic method coupled to the described DUS microsampling approach will be implemented (i) for workplace exposure controls aimed at feasibly and reliably monitoring the incidence of styrene and ethylbenzene vaporous in workroom environments (through the analysis of 1); (ii) to further investigate the possible use of compound 2 as a biomarker of both ovarian and cervical cancers; (iii) for in-depth investigations of specific tyrosinemic disorders (through the analysis of 3). Moreover, the developed chromatographic method will be applied to identify alimentary sources rich in (R)-2 being used as food and feed additives to limit microbial contaminations.

CRediT authorship contribution statement

Ina Varfaj: Methodology, Investigation, Writing – original draft. Michele Protti: Methodology, Investigation, Writing – original draft. Alessandro Di Michele: Investigation. Alceo Macchioni: Writing – review & editing. Wolfgang Lindner: Writing – review & editing, Supervision. Andrea Carotti: Conceptualization, Methodology, Validation, Formal analysis, Writing – original draft, Data curation. Roccaldo Sardella: Conceptualization, Methodology, Validation, Writing – original draft, Supervision, Writing – review & editing, Project administration. Laura Mercolini: Conceptualization, Methodology, Validation, Writing – original draft, Supervision, Writing – review & editing, Project administration.

Declaration of competing interest

The authors declare that they have no known competing financial interests or personal relationships that could have appeared to influence the work reported in this paper.

REFERENCES

[1] K. Tang, J. Yi, K. Huang, G. Zhang, Biphasic recognition chiral extraction: a novel method for separation of mandelic acid enantiomers, Chirality 21 (2009) 390e395.

[2] M. Terreni, G. Pagani, D. Ubiali, R. Fern andez-Lafuente, C. Mateo, J.M. Guis an, Modulation of penicillin acylase properties via immobilization techniques: one-pot chemoenzymatic synthesis of Cephamandole from Cephalosporin C, Bioorg. Med. Chem. Lett 11 (2001) 2429e2432.

[3] K. Str€om, J. Sj€ogren, A. Broberg, J. Schnürer, Lactobacillus plantarum MiLAB 393 produces the antifungal cyclic dipeptides cyclo(L-Phe-L-Pro) and cyclo(LPhe- trans-4-OH-L-Pro) and 3-phenyllactic acid, Appl. Environ. Microbiol. 68 (2002) 4322e4327.

[4] S.K. Bhatia, P.K. Mehta, R.K. Bhatia, T.C. Bhalla, Optimization of arylacetonitrilase production from Alcaligenes sp. MTCC 10675 and its application in mandelic acid synthesis, Appl. Microbiol. Biotechnol. 98 (2014) 83e94.

[5] A.D. Abell, J.W. Blunt, G.J. Foulds, M.H.G. Munro, Chemistry of the mycalamides: antiviral and antitumour compounds from a New Zealand marine sponge. Part 6.1e3 the synthesis and testing of analogues of the C(7)eC(10) fragment, J. Chem. Soc. Perkin Transact. 1 (1997) 1647e1654.

[6] J.P. Surivet, J.M. Vat ele, Total synthesis of antitumor Goniothalamus styryllactones, Tetrahedron 55 (1999) 13011e13028. [7] J. Mill, K.K. Schmiegel, W.N. Shaw, US Patent 4391826 (1983).

[8] S.S. Chaudhari, D.V. Gokhale, Phenyllactic Acid: a potential antimicrobial compound in lactic acid bacteria, J. Bacteriol. Mycol. Open Access 2 (2016) 121e125.

[9] X. Luo, Y. Zhang, L. Yin, W. Zheng, Y. Fu, Efficient synthesis of d-phenyllactic acid by a whole-cell biocatalyst co-expressing glucose dehydrogenase and a novel d-lactate dehydrogenase from Lactobacillus rossiae, 3 Biotech 10 (2020) 1e9.

[10] T. Fujita, H.D. Nguyen, T. Ito, S. Zhou, L. Osada, S. Tateyama, T. Kaneko, N. Takaya, Microbial monomers custom-synthesized to build true bio-derived aromatic polymers, Appl. Microbiol. Biotechnol. 97 (2013) 8887e8894.

[11] H. Kawaguchi, C. Ogino, A. Kondo, Microbial conversion of biomass into biobased polymers, Bioresour. Technol. 245 (2017) 1664e1673.

[12] W. Mu, S. Yu, L. Zhu, B. Jiang, T. Zhang, Production of 3-phenyllactic acid and 4-hydroxyphenyllactic

490 acid by Pediococcus acidilactici DSM 20284 fermentation, Eur. Food Res. Technol. 235 (2012) 581e585.
491 [13] H. Wang, H. Fan, H. Sun, L. Zhao, D. Wei, Process development for the production of (R)-(-)-mandelic
492 acid by recombinant Escherichia coli cells harboring nitrilase from Burkholderia cenocepacia J2315, Org.
493 Process Res. Dev. 19 (2015) 2012e2016.
494 [14] Y. Yang, F. Liu, Y. Wan, Simultaneous determination of 4-hydroxyphenyl lactic acid, 4-hydroxyphenyl
495 acetic acid, and 3,4-hydroxyphenyl propionic acid in human urine by ultra-high performance liquid
496 chromatography with fluorescence detection, J. Separ. Sci. 40 (2017) 2117e2122.
497 [15] J. Liu, A. Yan, Y. Yang, Y.Q. Wan, Determination of 4-hydroxyphenyllactic acid in human urine by
498 magnetic solid-phase extraction and high-performance anion-exchange chromatography with fluorescence
499 detection, Anal. Lett. 50 (2017) 259e270.
500 [16] E. Mayatepek, C.K. Seppel, G.F. Hoffmann, Increased urinary excretion of dicarboxylic acids and 4-
501 hydroxyphenyllactic acid in patients with Zellweger syndrome, Eur. J. Pediatr. 154 (1995) 755e756.
502 [17] F. Cosnier, H. Nunge, B. Cossec, L. Gat e, Simultaneous determination of aromatic acid metabolites of
503 styrene and styrene-oxide in rat urine by gas chromatography-Flame ionization detection, J. Anal. Toxicol.
504 36 (2012) 312e318.
505 [18] J.Z. Wang, X.J. Wang, Y.H. Tang, S.J. Shen, Y.X. Jin, S. Zeng, Simultaneous determination of mandelic
506 acid enantiomers and phenylglyoxylic acid in urine by high-performance liquid chromatography with
507 precolumn derivatization, J. Chromatogr. B Anal. Technol. Biomed. Life Sci. 840 (2006) 50e55.
508 [19] A. Tekewe, S. Singh, M. Singh, U. Mohan, U.C. Banerjee, Development and validation of HPLC method
509 for the resolution of drug intermediates: dl-3- Phenyllactic acid, dl-O-acetyl-3-phenyllactic acid and (±)-
510 mexiletine acetamide enantiomers, Talanta 75 (2008) 239e245.
511 [20] B.R. Lukito, Z. Wang, B. Sundara Sekar, Z. Li, Production of (R)-mandelic acid from styrene, L-
512 phenylalanine, glycerol, or glucose via cascade biotransformations, Bioresour. Bioprocess. 22 (2021) 2e11.
513 [21] Y. Zhu, Y. Wang, J. Xu, J. Chen, L. Wang, B. Qi, Enantioselective biosynthesis of L-phenyllactic acid by
514 whole cells of recombinant Escherichia coli, Molecules 22 (2017) 1e11.
515 [22] I. Jerkovi c, M. Roje, C.I.G. Tuberoso, Z. Marijanovi c, A. Kasum, M. Obradovi c, Bioorganic Research
516 of Galactites tomentosa Moench. Honey extracts: enantiomeric purity of chiral marker 3-Phenyllactic acid,
517 Chirality 26 (2014) 405e410.
518 [23] M. Shahnani, Y. Sefidbakht, S. Maghari, A. Mehdi, H. Rezadoost, A. Ghassempour, Enantioseparation of
519 mandelic acid on vancomycin column: experimental and docking study, Chirality 32 (2020) 1289e1298.
520 [24] P. Jandera, M. Skavrada, K. Klemmov a, V. Ba ckovsk a, G. Guiochon, Effect of the mobile phase on
521 the retention behaviour of optical isomers of carboxylic acids and amino acids in liquid chromatography on
522 bonded Teicoplanin columns, J. Chromatogr. A 917 (2001) 123e133.

[25] E. Müller, O. Sosedov, J.A.D. Gr€oning, A. Stolz, Synthesis of (R)-mandelic acid and (R)-mandelic acid amide by recombinant E. coli strains expressing a (R)- specific oxynitrilase and an arylacetonitrilase, Biotechnol. Lett. 43 (2021) 287e296.

[26] I. Ohhira, S. Kuwaki, H. Morita, T. Suzuki, S. Tomita, S. Hisamatsu, S. Sonoki, S. Shinoda, Identification of 3-Phenyllactic acid as a possible antibacterial substance produced by Enterococcus faecalis TH10, Biocontrol Sci. 9 (2004) 77e81.

[27] F. Ianni, Z. Pataj, H. Gross, R. Sardella, B. Natalini, W. Lindner, M. L€ammerhofer, Direct enantioseparation of underivatized aliphatic 3-hydroxyalkanoic acids with a quinine-based zwitterionic chiral stationary phase, J. Chromatogr. A 1363 (2014) 101e108.

[28] V. Mimini, F. Ianni, F. Marini, H. Hettegger, R. Sardella, W. Lindner, Electrostatic attraction-repulsion model with Cinchona alkaloid-based zwitterionic chiral stationary phases exemplified for zwitterionic analytes, Anal. Chim. Acta 1078 (2019) 212e220.

[29] I. Ilisz, A. Bajtai, A. P eter, W. Lindner, Cinchona Alkaloid-Based Zwitterionic chiral stationary phases applied for liquid chromatographic enantiomer separations: an overview, Methods Mol. Biol. 1985 (2019) 251e277.

[30] R. Sardella, A. Carotti, G. Manfroni, D. Tedesco, A. Martelli, C. Bertucci, V. Cecchetti, B. Natalini, Enantioresolution, stereochemical characterization and biological activity of a chiral large-conductance calcium-activated potassium channel opener, J. Chromatogr. A 1363 (2014) 162e168.

[31] B. Cerra, A. Carotti, D. Passer, R. Sardella, G. Moroni, A. Di Michele, A. Macchiarulo, R. Pellicciari, A. Gioiello, Exploiting chemical toolboxes for the expedited generation of tetracyclic quinolines as a novel class of PXR agonists, ACS Med. Chem. Lett. 10 (2019) 677e681.

[32] L. Mercolini, M. Protti, Biosampling strategies for emerging drugs of abuse: towards the future of toxicological and forensic analysis, J. Pharmaceut. Biomed. Anal. 130 (2016) 202e219.

[33] L. Mercolini, M.A. Saracino, M. Protti, Current advances in biosampling for therapeutic drug monitoring of psychiatric CNS drugs, Bioanalysis 7 (2015) 1925e1942.

[34] A.C. Evans, A.S. Petit, S.G. Guillen, A.J. Neukirch, S. V Hoffmann, N.C. Jones, Chiroptical characterization tools for asymmetric small molecules - experimental and computational approaches for electronic circular dichroism (ECD) and anisotropy spectroscopy, RSC Adv. 11 (2021) 1635e1643.

[35] P.J. Stephens, F.J. Devlin, C.F. Chabalowski, M.J. Frisch, Ab-initio calculation of vibrational absorption and circular-dichroism spectra using densityfunctional force-fields, J. Phys. Chem. 98 (1994) 11623e11627.

[36] J.D. Chai, M. Head-Gordon, Long-range corrected hybrid density functionals with damped atomeatom dispersion corrections, Phys. Chem. Chem. Phys. 10 (2008) 6615e6620.

[37] A.E. Hansen, K.L. Bak, Ab initio calculations and display of enantiomeric and nonenantiomeric

556 anisotropic circular Dichroism: the lowest p / p* excitation in butadiene, cyclohexadiene, and methyl-
557 substituted cyclohexadiene, J. Phys. Chem. A 104 (2000) 11362e11370.
558 [38] J. Autschbach, T. Ziegler, S.J.A. Van Gisbergen, E.J. Baerends, Chiroptical properties from time-
559 dependent density functional theory. I. Circular dichroism spectra of organic molecules, J. Chem. Phys. 116
560 (2002) 6930e6940.
561 [39] C. Bannwarth, S. Grimme, A simplified time-dependent density functional theory approach for
562 electronic ultraviolet and circular dichroism spectra of very large molecules, Comput. Theor. Chem. 1040
563 (2014) 45e53.
564 [40] F. Neese, The ORCA program system, Wires Comput. Mol. Sci. 2 (2012) 73e78. [41] P.J. Stephens, N.
565 Harada, ECD cotton effect approximated by the Gaussian curve and other methods, Chirality 22 (2010)
566 229e233.
567 [42] T. Bruhn, A. Schaumloffel, Y. Hemberger, G. Bringmann, SpecDis: quantifying the Comparison of
568 calculated and experimental electronic circular dichroism spectra, Chirality 25 (2013) 243e249.
569 [43] R. Sardella, A. Macchiarulo, F. Urbinati, F. Ianni, A. Carotti, M. Kohout, W. Lindner, A. Peter, I. Ilisz,
570 Exploring the enantiorecognition mechanism of Cinchona alkaloid-based zwitterionic chiral stationary
571 phases and the basic trans-paroxetine enantiomers, J. Separ. Sci. 41 (2018) 1199e1207.
572 [44] W.G. Hoover, Canonical dynamics: equilibrium phase-space distributions, Phys. Rev. A 31 (1985)
573 1695e1697.
574 [45] S. Nos e, A unified formulation of the constant temperature molecular dynamics methods, J. Chem.
575 Phys. 81 (1984) 511e519.
576 [46] D.E. Shaw, A fast, scalable method for the parallel evaluation of distancelimited pairwise particle
577 interactions, J. Comput. Chem. 26 (2005) 1318e1328.
578 [47] A. Carotti, F. Ianni, S. Sabatini, A. Di Michele, R. Sardella, G.W. Kaatz, W. Lindner, V. Cecchetti, B.
579 Natalini, The "racemic approach" in the evaluation of the enantiomeric NorA efflux pump inhibition activity
580 of 2-phenylquinoline derivatives, J. Pharmaceut. Biomed. Anal. 129 (2016) 164e173.
581 [48] N. Grecs o, M. Kohout, A. Carotti, R. Sardella, B. Natalini, F. Fül€op, W. Lindner, A. P eter, I. Ilisz,
582 Mechanistic considerations of enantiorecognition on novel Cinchona alkaloid-based zwitterionic chiral
583 stationary phases from the aspect of the separation of trans-paroxetine enantiomers as model compounds,
584 J. Pharmaceut. Biomed. Anal. 124 (2016) 164e173.
585 [49] C.V. Hoffmann, R. Pell, M. L€ammerhofer, W. Lindner, Synergistic effects on enantioselectivity of
586 zwitterionic chiral stationary phases for separations of chiral acids, bases, and amino acids by HPLC, Anal.
587 Chem. 80 (2008) 8780e8789.
588 [50] F. Ianni, A. Carotti, M. Marinozzi, G. Marcelli, A. Di Michele, R. Sardella, W. Lindner, B. Natalini,

589 Diastereo- and enantioseparation of a Na-Boc amino acid with a zwitterionic quinine-based stationary
590 phase: focus on the stereo recognition mechanism, Anal. Chim. Acta 885 (2015) 174e182.
591 [51] I. Ilisz, N. Grecs o, A. Aranyi, P. Suchotin, D. Tymecka, B. Wilenska, A. Misicka, F. Fül€op, W. Lindner, A.
592 P eter, Enantioseparation of b2-amino acids on cinchona alkaloid-based zwitterionic chiral stationary
593 phases. Structural and temperature effects, J. Chromatogr. A 1334 (2014) 44e54.
594 [52] C. Calder on, J. Horak, M. L€ammerhofer, Chiral separation of 2-hydroxyglutaric acid on cinchonan
595 carbamate based weak chiral anion exchangers by highperformance liquid chromatography, J. Chromatogr.
596 A 1467 (2016) 239e245.
597 [53] C. Calder on, M. L€ammerhofer, Chiral separation of short chain aliphatic hydroxycarboxylic acids on
598 cinchonan carbamate-based weak chiral anion exchangers and zwitterionic chiral ion exchangers, J.
599 Chromatogr. A 1487 (2017) 194e200.
600 [54] A. Bajtai, I. Ilisz, A. P eter, W. Lindner, Liquid chromatographic resolution of natural and racemic
601 Cinchona alkaloid analogues using strong cation- and zwitterion ion-exchange type stationary phases.
602 Qualitative evaluation of stationary phase characteristics and mobile phase effects on stereoselectivity and
603 retention, J. Chromatogr. A 1609 (2020) 460498.
604 [55] C.V. Hoffmann, R. Reischl, N.M. Maier, M. L€ammerhofer, W. Lindner, Stationary phase-related
605 investigations of quinine-based zwitterionic chiral stationary phases operated in anion-, cation-, and
606 zwitterion-exchange modes, J. Chromatogr. A 1216 (2009) 1147e1156.
607 [56] I. Ilisz, A. Bajtai, W. Lindner, A. P eter, Liquid chromatographic enantiomer separations applying chiral
608 ion-exchangers based on Cinchona alkaloids, J. Pharmaceut. Biomed. Anal. 159 (2018) 127e152.
609 [57] G. Lajk o, N. Grecs o, G. T oth, F. Fül€op, W. Lindner, I. Ilisz, A. P eter, Liquid and subcritical fluid
610 chromatographic enantioseparation of Na-Fmoc proteinogenic amino acids on Quinidine-based zwitterionic
611 and anion-exchanger type chiral stationary phases. A comparative study, Chirality 29 (2017) 225e238.
612 [58] I. Ilisz, N. Grecs o, A. Misicka, D. Tymecka, L. L az ar, W. Lindner, A. P eter, Comparison of the
613 separation performances of cinchona alkaloid-based zwitterionic stationary phases in the
614 enantioseparation of b2- and b3-amino acids, Molecules 20 (2015) 70e87.
615 [59] D. Tan acs, T. Orosz, I. Ilisz, A. P eter, W. Lindner, Unexpected effects of mobile phase solvents and
616 additives on retention and resolution of N-Acyl-D,LLeucine applying cinchonane-based chiral ion
617 exchangers, J. Chromatogr. A 1648 (2021) 462212.
618 [60] R. Pell, S. Si c, W. Lindner, Mechanistic investigations of cinchona alkaloidbased zwitterionic chiral
619 stationary phases, J. Chromatogr. A 1269 (2012) 287e296.
620 [61] F. Ianni, R. Sardella, A. Carotti, B. Natalini, W. Lindner, M. L€ammerhofer, Quinine-based zwitterionic
621 chiral stationary phase as a complementary tool for peptide analysis: mobile phase effects on enantio- and

622 stereoselectivity of underivatized oligopeptides, Chirality 28 (2016) 5e16.
623 [62] L.O. Zamir, R. Tiberi, K.A. Devor, F. Sauriol, S. Ahmad, R.A. Jensen, Structure of D-prephenyllactate a
624 carboxycyclohexadienyl metabolite from neurospora crassa, J. Biol. Chem. 33 (1988) 17284e17290.
625 [63] American Conference of Governmental Industrial Hygienists, Threshold Limit Values for Chemical
626 Substances and Physical Agents and Biological Indices, American Conference of Governmental Industrial
627 Hygienists, Cincinnati, 1991.
628 [64] A.R. Choi, S.G. Im, M.Y. Lee, S.H. Lee, Evaluation of the suitability of establishing biological exposure
629 indices of styrene, Safe. Health. Work 10 (2019) 103e108.
630 [65] European Medicines Agency (EMA), Committee for Medicinal Products for Human Use (CHMP),
631 Guideline on Bioanalytical Method Validation, EMEA/ CHMP/EWP/192217/2009, London, UK, 2011.
632

Supplementary Material

Efficient enantioresolution of aromatic α-hydroxy acids with *Cinchona* alkaloid-based zwitterionic stationary phases and volatile polar-ionic eluents

Ina Varfaj[1a], Michele Protti[2a], Alessandro Di Michele[3], Alceo Macchioni[4], Wolfgang Lindner[5], Andrea Carotti[1]*, Roccaldo Sardella[1,6]*, Laura Mercolini[2]

[1]*Department of Pharmaceutical Sciences, University of Perugia, Via Fabretti 48, 06123 - Perugia, Italy.*

[2]*Department of Pharmacy and Biotechnology (FaBiT), Alma Mater Studiorum, University of Bologna, Via Belmeloro 6, 40126 - Bologna, Italy.*

[3]*Department of Physics and Geology, University of Perugia, Via Pascoli 1, 06123 - Perugia, Italy*

[4]*Department of Chemistry, Biology and Biotechnology, University of Perugia, Via Elce di Sotto 8, 06123 - Perugia, Italy.*

[5]*Department of Analytical Chemistry, University of Vienna, Währinger Strasse 38, 1090 - Vienna, Austria.*

[6]*Center for Perinatal and Reproductive Medicine, University of Perugia, Santa Maria della Misericordia University Hospital, 06132 Perugia, Italy.*

[a] Ina Varfaj and Michele Protti contributed equally to this work.

*Corresponding authors:

Andrea Carotti, email: andrea.carotti@unipg.it

Roccaldo Sardella, email: roccaldo.sardella@unipg.it

Figure 1S. Chromatograms of compound 2 obtained with CSP 2 [CHIRALPAK® ZWIX(+), from Chiral Technology Europe - Strasbourg, France) under the optimal [ACN/MeOH 95/5 (v/v) with 80 mM FA] mobile phase composition and experimental conditions: eluent flow rate, 0.2 mL/min; column temperature, 25 °C; detection wavelength, 254 nm.

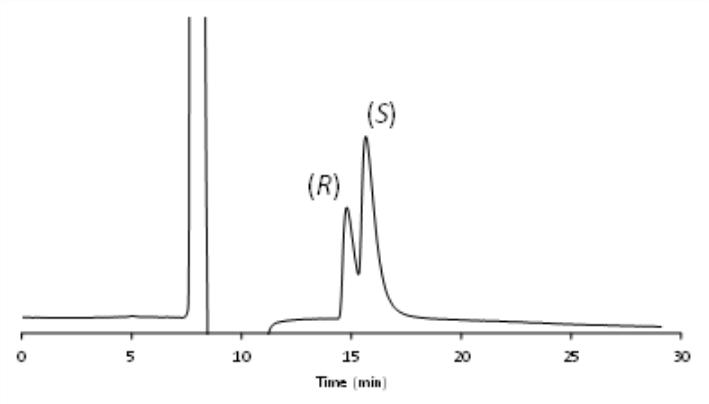

Figure 2S. Experimental ECD spectra of the first- (blue line) and second-eluted (red line) enantiomeric fraction of (A) compound **1** and (B) compound **2**. The theoretical spectrum of the (*S*)-enantiomer is reported as black dashed-line.

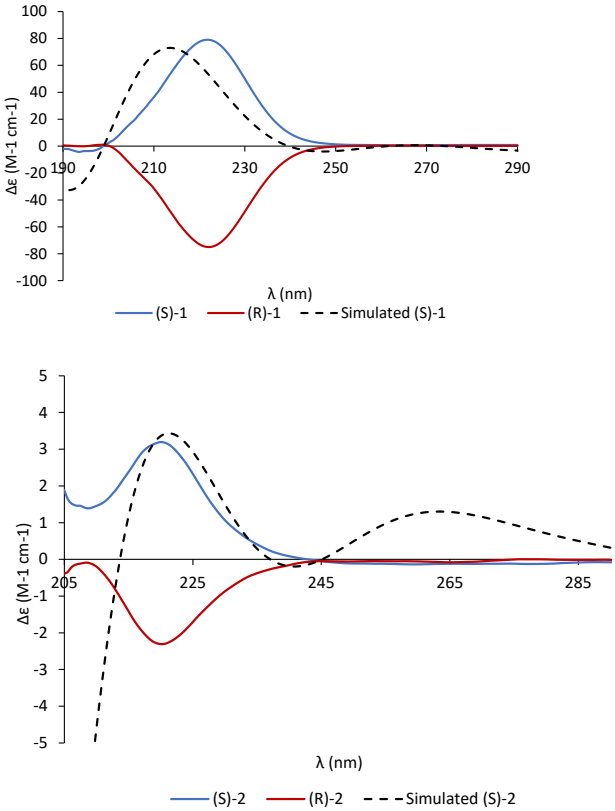

633

Figure 3S. ESI-UHPLC-MS chromatogram obtained from the analysis of a DUS sample spiked with *rac*-**1** (on-spot concentration: 100 ng/mL). Extracted ion: *m/z* 151.17.